PSFC/JA-04-8

Studies of the 1.5-MW, 110-GHz Gyrotron Experiment

Anderson, J. P., Shapiro, M. A., Temkin, R. J., Mastovsky, I., Cauffman, S.*

June 2004

Plasma Science and Fusion Center
Massachusetts Institute of Technology
Cambridge, MA 02139 USA

* Microwave Power Products Division
Communications and Power Industries
Palo Alto, CA 94303 USA

Studies of the 1.5-MW, 110-GHz Gyrotron Experiment

James P. Anderson, Michael A. Shapiro, Richard J. Temkin, *Fellow, IEEE*, I. Mastovsky, and S. Cauffman*

Plasma Science and Fusion Center, Massachusetts Institute of Technology, Cambridge, MA 02139

*Microwave Power Products Division, Communications and Power Industries, Palo Alto, CA 94303

Abstract--**Results of a 1.5 MW, 110 GHz short (3 μs) pulse gyrotron experiment are reported. The gyrotron magnetron injection gun operated at full voltage (96 kV) and current (40 A), producing up to 1.4 MW at 110 GHz in the $TE_{22,6}$ mode. The operation of the $TE_{22,6}$ mode, as well as nearby modes, was measured as a function of magnetic field at the cavity and at the electron gun to produce a mode map. Significant mode competition was found, but the measured efficiency of 37 % in the $TE_{22,6}$ mode, without a depressed collector, is close to the design value of 39 %. The beam alpha, the ratio of transverse to axial velocity in the electron beam, was measured with a probe. The alpha value was found to be 1.33 when the gyrotron was operating at conditions for achieving the highest output power level (1.4 MW.) This value of alpha is less than the design value of 1.4, possibly accounting for the slightly reduced experimental efficiency. The output power and efficiency, as a function of magnetic field, beam voltage, and beam current, are in good agreement with nonlinear theory and simulations with the MAGY code. These results are promising for the development of an industrial version of this gyrotron capable of long pulse or CW operation.**

I. INTRODUCTION

Gyrotron oscillators, high power microwave sources which operate based on the cyclotron resonance maser (CRM) instability, have numerous applications. Fusion devices, in particular, have a need for high power microwave tubes to provide high power plasma heating. Multi-megawatt plasma heating is currently being carried out in numerous plasma experiments, such as the DIII-D tokamak at General Atomics [1], the Large Helical Device (LHD) at the NIFS in Japan [2], the JT-60 tokamak at JAERI in Japan [3], the TCV tokamak in Lausanne, Switzerland [4], and the ASDEX tokamak in Garching, Germany [5].   A ten

megawatt heating system is planned for the Wendelstein 7X stellerator and a 27 MW system for the proposed ITER machine. All of these devices currently use, or plan to use, gyrotrons for electron cyclotron resonance heating (ECRH) and electron cyclotron current drive (ECCD).

For the Wendelstein 7X stellerator, 140 GHz gyrotrons have been built which currently provide over 500 kW for pulses of several minutes and 1 MW for about 10 s [6][7]. The DIII-D tokamak at General Atomics is using three 1 MW, 110 GHz gyrotrons operating at up to 10 s pulse lengths [8]. In addition, a gyrotron generating high power at 170 GHz is currently under development for providing the heating system for the ITER reactor, which will ultimately require a large array of gyrotrons [9].

For these heating systems requiring about 10 MW or more, it would be advantageous to increase the power-per-tube ratio to the 1.5 to 2 MW range. It is with this goal in mind that the US gyrotron program began working on the development of a 1.5 MW, 110 GHz gyrotron in 1999 [10]. This design is based on extending the successful 1 MW design with a new cavity, a new electron gun for higher voltage (96 kV), and with a single-stage or two-stage [11] depressed collector for higher net efficiency. To validate the new design, MIT has built an experimental, short-pulse version of the tube, which is described here. Progress is also being made worldwide on higher power gyrotrons. Coaxial gyrotrons, for example, have been built in Europe with 2.2 MW of output at 165 GHz, currently operating in short pulses [12]. A long pulse / CW version of this tube is being planned. In Japan, an experimental 110 GHz gyrotron tube has been operated at up to 1.2 MW for 4 seconds [13], and is being tested at up to 1.5 MW. In Russia, output power levels above 1 MW have been obtained in a coaxial gyrotron at a frequency of 140 GHz [14]. A 170 GHz gyrotron has demonstrated up to 1.5 MW in short pulse operation in the $TE_{28,8}$ mode at MIT [15].

The main goal of the experiment presented here is to examine such issues as mode competition, output power, mode purity, mode start-up scenarios, changes in the beam velocity ratio, and the operating regions of neighboring modes for the US 1.5-MW 110-GHz gyrotron. In 2002, we reported on the initial successful short-pulsed operation of the experiment using an older triode gun. That experiment, although limited due to the use of a gun not designed specifically for the experiment, provided some encouraging preliminary results, with over 1 MW of output power obtained [16]. A new diode gun has since replaced the triode gun. This new gun, which had previously been separately tested for emission uniformity [17], has been rebuilt with a new cathode.

This paper will first describe the setup of the experiment, show the results obtained using the new gun, and compare them with theory and simulation, and then discuss these results, along with plans for future experiments.

II. Design

The crucial design issues of a multi-megawatt gyrotron involve the essential elements of the gyrotron: the gun and the cavity. The gun for this experiment has been designed to produce a 40 A electron beam at 96 kV with the aid of ray tracing codes such as EGUN [18]. In addition, the electron gun geometry has been optimized to yield a beam with low velocity spread. The cavity has been designed using linear start-up theory and nonlinear gyrotron theory, along with a code which self-consistently solves the beam/wave interaction equations [19]. It has been extensively simulated as well through the use of a multi-mode code developed by the University of Maryland called MAGY [20]. This cavity profile is crucial in minimizing mode competition and limiting ohmic losses, and is designed to produce a single high-purity output mode.

Frequency	110 GHz
Microwave Power	1.5 MW
Beam Voltage	96 kV
Beam Current	40 A
Beam Alpha ($\alpha = v_\perp / v_\parallel$)	1.4
Operating Mode	$TE_{22,6}$
Pulse Length	3 μs
Cavity Magnetic Field	4.3 T
Efficiency (w/o Dep. Coll.)	39%
Efficiency (w. Dep. Coll.)	> 50%

Table 1. The design parameters are listed for the 1.5-MW, 110-GHz gyrotron.

The design parameters for the gyrotron, listed in Table 1, are chosen such that a 96 kV, 40 A electron beam generates 1.5 MW of power in the $TE_{22,6}$ cylindrical waveguide mode, corresponding to an efficiency of 39 %. The $TE_{22,6}$ mode was chosen for several reasons. First, the points of highest intensity (the first Bessel function maxima) of the mode pattern are away from the walls of the structure, towards the center of the cavity. This is an important design characteristic since the ohmic wall losses and heating are minimized with such a mode. Second, theory and simulation have shown that this mode provides high coupling with the beam, such that it is a highly efficient mode for energy transfer. Third, the distribution of modes in the frequency spectrum suggests that the $TE_{22,6}$ mode is fairly isolated from other modes, implying a stable operating region without much mode competition. Finally, we have previous experience with other tubes

which use the $TE_{22,6}$ mode, including the robust 1 MW, 110 GHz gyrotron, upon which this experiment is based. These tubes have been highly successful in the past.

The alpha, α, is a beam parameter measuring the ratio of the perpendicular velocity of electrons to the parallel velocity. The beam alpha is a useful parameter since it indicates how much rotational (perpendicular) energy is available for mode excitation. If the alpha is small, there is little energy transfer in the interaction region since most of the electron energy is axial. However, it is very difficult to fabricate an electron gun capable of producing high alpha with low velocity spread. If the design value of the alpha is too large, then imperfections in beam uniformity, alignment, and/or velocity spread can result in some electrons being reflected back toward the gun. The designed alpha for this experiment is 1.4 at the cavity with a perpendicular velocity spread ($\delta v_\perp / v_\perp$) of 2.5 % from optical sources. (For a discussion of other sources of velocity spread, see [17].)

III. EXPERIMENTAL SETUP

The schematic for the short-pulsed axial configuration experiment is shown in Figure 1. The electron gun in this case is a diode gun. A gate valve is located between the gun and the rest of the tube to allow rapid changes to be made to the experiment while maintaining vacuum conditions for the gun. The superconducting magnet is able to produce 4.3 T at its center, where the cavity is located to take advantage of the flat field profile. In addition, a magnetic coil is placed at the cathode location. This gun coil provides an additional small field at the cathode which has two effects. Both the alpha and beam radius are altered by changing the compression ratio, so the gun coil may be used to fine-tune these two beam parameters. The microwave resonator, as mentioned previously, is an open ended cylindrical cavity, with a linear downtaper from the beam tunnel and a rounded uptaper to the output waveguide. This cavity has been designed based on cold-cavity codes, which solve for the electromagnetic fields in the absence of the electron beam, such that the $TE_{22,6}$ mode resonates at 110 GHz with a quality factor, Q, of 935. Figure 2 shows the wall profile and cold-cavity field profile for the $TE_{22,6}$ mode. Although it is not shown in the schematic, an alpha probe [21] is located immediately before the cavity. The collector, in this configuration where the power is extracted axially, is a hollow copper pipe which also acts as a cylindrical overmoded waveguide which guides the generated microwaves to a window at the end of the tube. The

fused-quartz window is of a thickness designed to allow full transmission at the mode bounce angle at 110 GHz. Most of the power is radiated in a directed cone determined by the bounce angle of the wave.
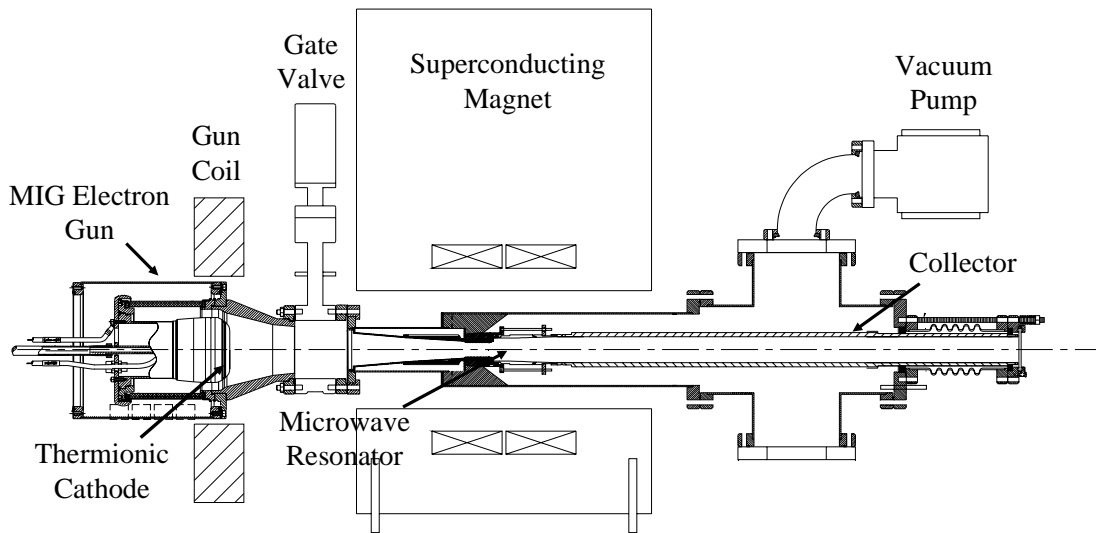

Figure 1. A schematic shows the 1.5-MW, 110-GHz gyrotron oscillator experiment in its axial configuration.

The position of the tube must be carefully adjusted in order to make sure the cavity is properly aligned with respect to the beam and magnetic field. The gyrotron has freedom of movement in the horizontal and vertical directions at both the collector end and the gun end of the tube. The tube position may be axially adjusted as well.

There are several diagnostics we use to take measurements of the axial configuration gyrotron experiment. To measure the power, a calibrated calorimeter placed near the output window is used. This calorimeter indicates the averaged power heating its surface over the duty cycle, typically 1 s. The pulse shape and duration is measured by a horn antenna fed to a power detecting diode located at a distance and angle from the window. Including the relative error in the pulse width, the relative error for the power measurement is ± 5 %. A horn and waveguide network is also used to deliver output radiation to a heterodyne receiver system. This system, composed of a local oscillator, harmonic mixer, and filters, allows us to measure the frequency content of the output. By tuning the local oscillator, a broad range of frequencies may be scanned with very high accuracy (± 10 MHz). Finally, the alpha probe, a small annular metal ring which measures an induced electric potential from the radial electric field of the beam, is used to

estimate the beam velocity ratio near the cavity, where the alpha is unchanging. This type of probe has been used successfully in previous experiments [15]. The accuracy of the calibrated alpha probe is ± 10 %.
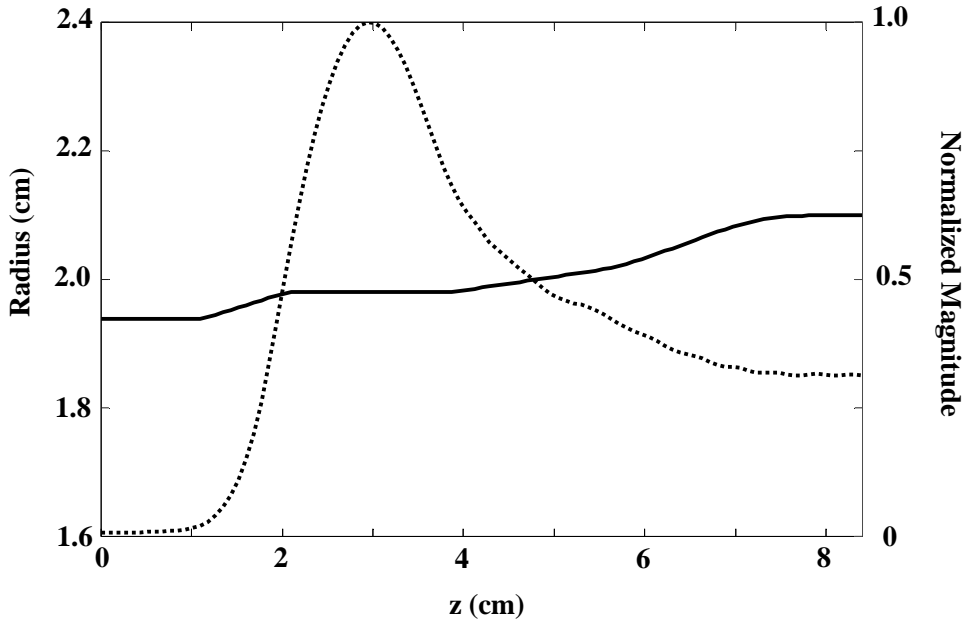

Figure 2. The cavity profile is shown by the solid line. The dotted line represents the field structure. For the TE$_{22,6}$ mode, the resonant cold-cavity frequency is 110.08 GHz, and the Q is 935.

IV. EXPERIMENTAL RESULTS

Initial results of the axial experiment shown in Figure 1 were obtained in 2002 using a triode electron gun from an earlier gyrotron tube at MIT [16]. This gun was used with the 170 GHz experiment which demonstrated 1.5 MW of power in the TE$_{28,8}$ mode [15]. For the 110 GHz gyrotron experiment, the gun operated at 82 kV and 50 A. The main goal of this brief experiment was to test the cavity design. The tube, after only a cursory alignment, demonstrated over 1 MW of power at a frequency near 110 GHz, corresponding to an efficiency of 25 %. The results, although preliminary, were very promising for future experiments.

Subsequent to those initial investigations, the gun was replaced by the 96 kV, 40 A diode gun. This gun, unlike the earlier triode gun, was designed specifically for the present 110 GHz experiment, producing an electron beam with parameters which match those listed in Table 1.

The tube was fixed at a location which provided optimal power by aligning the tube in the magnet. After this alignment had been accomplished, the goal of the first part of the experiment was to locate the

modes and their frequencies by varying the operating parameters. A list of some of the frequencies of the radiation measured by the receiver system and their corresponding modes is provided in Table 2. The frequencies were also compared with the resonating frequencies in the cavity geometry predicted by cold-cavity electromagnetic theory. The majority of measured frequencies were very close to the predicted values, as shown by the table.

Mode	f_{thy} (GHz)	f_{meas} (GHz)
TE$_{17,7}$	103.55	103.64
TE$_{18,7}$	106.60	106.70
TE$_{21,6}$	107.14	107.15
TE$_{19,7}$	109.63	109.70
TE$_{22,6}$	**110.08**	**110.08**
TE$_{20,7}$	112.64	112.65
TE$_{23,6}$	113.01	113.01
TE$_{21,7}$	115.64	115.65
TE$_{22,7}$	118.63	118.64

Table 2. A list of measured frequencies is compared with cold-cavity theory.

The next part of the experiment was to note the regions of parameter space in which the various possible excitation modes are observed. This "mode map" locates the operational limits of each mode and identifies the nearest competing modes at these limits. For the typical mode map two parameters are varied, e.g. the main magnetic field and the cathode magnetic field. The field at the cavity affects the cyclotron frequency of the electrons in the beam, on which the detuning parameter for the excited mode is based, and also affects the beam radius and the beam alpha. Changing the cavity magnetic field will thus affect the interaction efficiency, and can also cause a shift from one mode and frequency of operation to another. The magnetic field at the cathode, which is fine-tuned by adjusting the gun coil current, affects the beam alpha, as well as the beam radius. These effects can limit the effective operating region of the device. According to adiabatic theory, the beam alpha increases as the cathode field decreases, since

$$\alpha = \left(\frac{\gamma^2 - 1}{\gamma^2 \beta_\perp^2} - \frac{1}{\gamma^2} \right)^{-1/2} \tag{1}$$

where γ is the relativistic factor dependent on the accelerating voltage of the beam, and the perpendicular velocity component, $\beta_\perp$, is given by

$$\beta_\perp = \left(\frac{E_g}{cB_g} \right) \sqrt{\frac{B_o}{B_g}} \tag{2}$$

Here E_g and B_g are the electric and magnetic fields at the gun cathode, and B_o is the cavity magnetic field. Eventually the alpha may become so high that the electrons begin to reflect back into the gun. In addition, adjusting the magnetic compression ratio affects the beam radius, causing the mode to change, and the beam radius may become so large that interception may occur with the walls.

The mode map shown in Figure 3 shows the location of the design $TE_{22,6}$ mode as well as several nearby modes. During these measurements, the beam voltage and current were maintained at 96 kV and 40 A. The $TE_{21,6}$, $TE_{22,6}$ and $TE_{23,6}$ modes all appear in a band of modes following a linear upward slope. Likewise the $TE_{19,7}$ and $TE_{20,7}$ modes lie along a line, although they are located underneath the $TE_{m,6}$ modes (m = 21-23). In addition, the points of highest efficiency are located for several modes. These generally occur at the lower limits of the cavity magnetic field where the mode is still excited. For the regions on the mode map where the cathode magnetic field is low, the alpha is high and the beam reflects so there is no stable operation. Above the band of modes, where the cathode magnetic field is high, the body current increases, indicating that beam interception is occurring. For other regions on the mode map where no modes are labeled there is unstable mode operation, or oscillation between two or more modes.
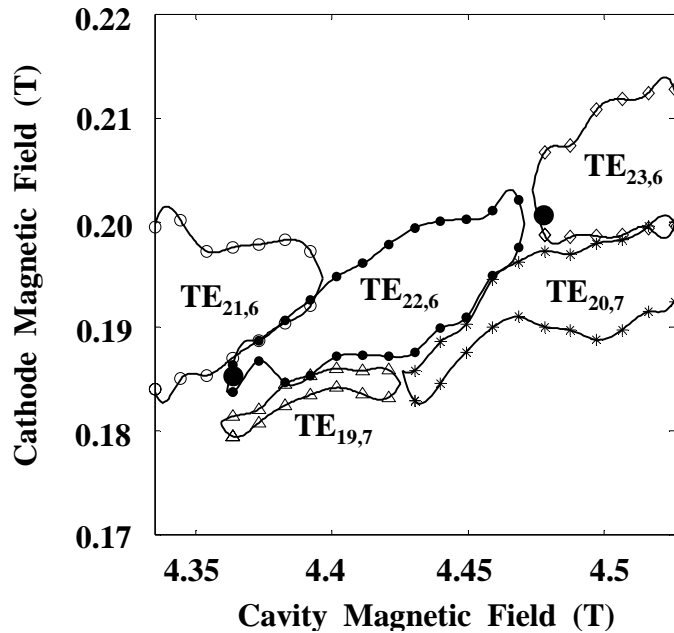

Figure 3. The mode map is shown for the design mode and nearby competing modes. Also included are the points of highest measured mode efficiency.

The power and efficiency were extensively measured for the $TE_{m,6}$ modes. For these scans a calorimeter was used to estimate the average power as the main magnetic field was swept, and the

efficiency calculated based on a beam voltage and current of 96 kV and 40 A. The pulse length used to calculate the actual power was typically around 2.6 µs. An example of a flat-top pulse shape measured by the power diode is shown in Figure 4. For each data point in Figure 5, the cathode magnetic field was adjusted such that the mode exhibited the largest amount of power. As plotted in Figure 5, the $TE_{21,6}$ and $TE_{23,6}$ modes each produced a maximum of 1.1 MW, corresponding to an efficiency of around 30 %. The highest power in the design mode was a little more than 1.4 MW, with 37 % efficiency. This data point corresponds with the point of highest efficiency marked in Figure 3. The multi-mode gyrotron simulation tool MAGY was used to generate simulated results for the $TE_{22,6}$ mode over several magnetic field values. These results are overlaid on the figure for comparison. The experimental results agreed well with the simulation, indicating that the cavity was aligned properly within the magnet, and that the gun was operating at close to the design parameters. It should be noted, however, that these particular simulations do not include the effects of emission nonuniformity, although this effect has been studied [22].
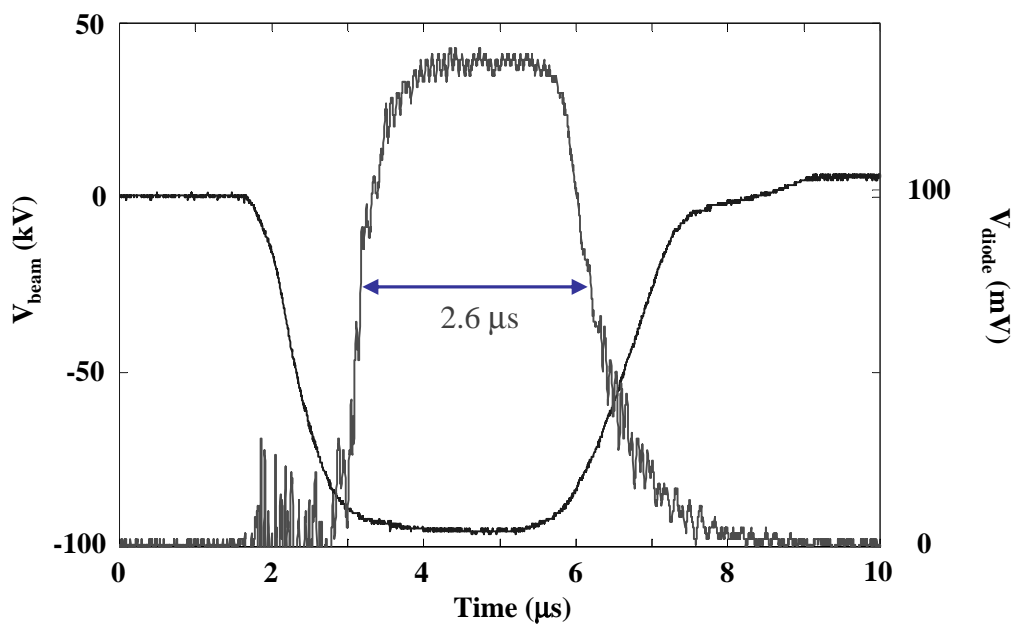

Figure 4. The voltage pulse shape is shown for a beam voltage of 96 kV. The power diode output is also shown. For this trace, the pulse width is 2.6 µs.
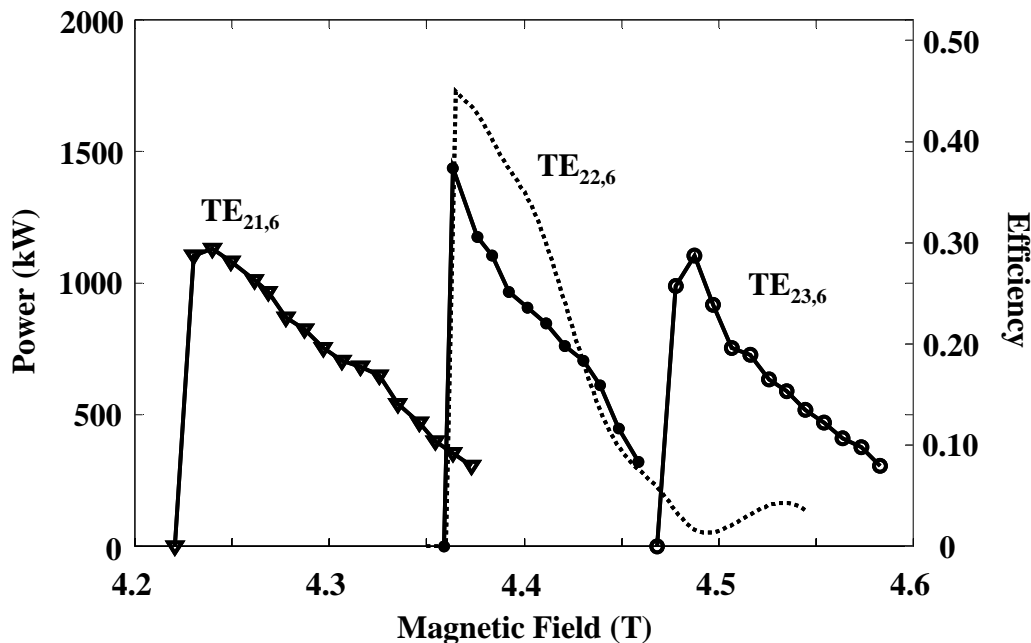
Figure 5. A power scan of three $TE_{m,6}$ modes is plotted for various magnetic field values. A comparison with MAGY simulations is given for the $TE_{22,6}$ mode (dotted line).

The beam alpha was determined based on voltage measurements from the calibrated alpha probe, the beam voltage, and the beam current. The alpha probe data taken for the magnetic field sweep of the $TE_{22,6}$ mode are plotted in Figure 6. Also shown is the alpha calculated from adiabatic theory using the same parameters based on the EGUN simulation results at $\alpha = 1.43$. The measured alpha for each operating point was very close to the calculated value. The point of highest efficiency, at $B = 4.36$ T, corresponded to a calculated alpha of 1.45, while the measured alpha was around 1.33. At $\alpha = 1.33$, the theoretical efficiency is predicted to be 36.4 %. MAGY results at the lower alpha were not available at the time of publication, but a study is currently being done at MIT using MAGY with inputs that match the beam parameters measured in the experiment.
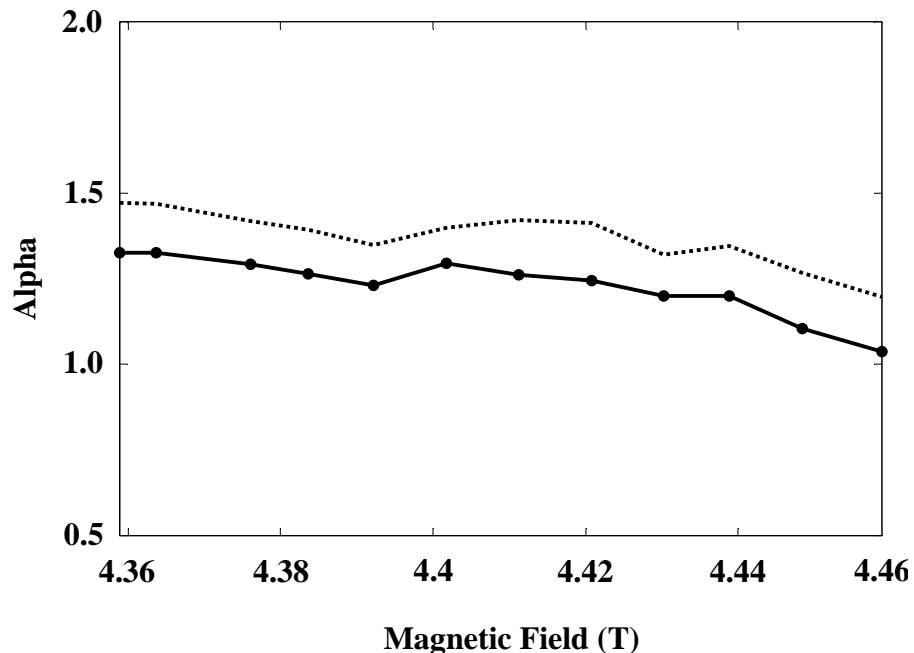
Figure 6. The alpha values are shown by the solid line as measured by the alpha probe for a range of magnetic field values. The alpha values computed based on EGUN results are indicated by the dotted line.

Once the optimal magnetic field values were identified for excitation of the desired mode, the effects of varying other operating parameters, such as the beam voltage and current, could be explored. These parameters were varied to determine the range of values over which the desired mode would be excited, and to determine the operating point with optimal efficiency. In one experiment, once the $TE_{22,6}$ mode was located at 96 kV and 40 A, and the magnetic field was fixed at 4.4 T to stabilize the mode, with a beam alpha of 1.2, the current was slowly decreased. The decrease in power was recorded and plotted in Figure 7(a). A comparison with MAGY for this magnetic field value is also provided. The slight discrepancy in power levels between the experimental results and MAGY are due to the fact that the beam alpha for the experiment at this operating point differs from the alpha used in the simulations. In Figure 7(b), the results of a similar experiment are shown, except this time the current was fixed, while the voltage was decreased until the mode power was negligible. While MAGY predicted the $TE_{22,6}$ mode would appear around 68 kV, the beginning voltage measured in the experiment was 75 kV, although this may also be explained by the difference in the alpha measured in the experiment and the alpha used in the simulations.
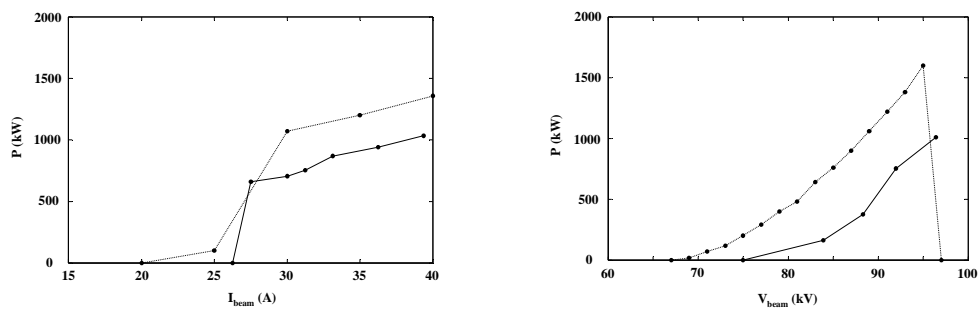
Figure 7. A scan was taken of the power and efficiency as a function of current for the $TE_{22,6}$ mode (a). For this particular plot, $V_b = 96$ kV and B = 4.4 T. The MAGY results are shown by the dotted line. A similar plot was generated to determine the variation of power and efficiency with voltage (b). The MAGY simulations are shown by the dotted line. Here $I_b = 40$ A and B = 4.4 T.

Related to this last experiment was one which measured the mode content and alpha as the voltage was varied. In this study, the $TE_{22,6}$ mode was first optimized at 96 kV, and 40 A, with a magnetic field of 4.4 T. For this magnetic field, the beam alpha at 96 kV, 40 A operation was measured by the alpha probe as 1.2. The voltage was then varied while the mode frequency and beam alpha were monitored. The results are shown in Figure 8, which also contains start-up current contours for a beam current of 40 A, as determined by linear start-up theory for an idealized Gaussian field profile in the cavity. Both the $TE_{21,6}$ mode and the $TE_{23,6}$ mode were measured as the voltage was varied. The limits of mode operation were found to match well with theory.
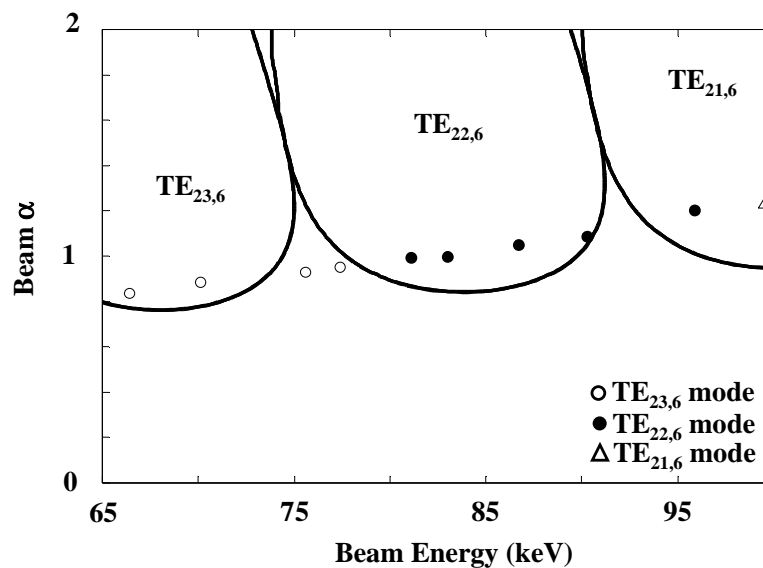

Figure 8. A plot is shown of the measured beam alpha and mode content as the beam voltage is varied when B = 4.4 T. The beam alpha is around 1.2 at 96 kV for this set of operating parameters. Also shown are the start-up contours of the modes for I = 40 A.

V. DISCUSSION

The design issues addressed in this experiment include the identification of various modes near the design mode, the operational limits of the design mode, its start-up conditions, the location of competing modes, and the beam alpha. In all cases, the measured results have been compared with theoretically predicted values or values obtained with numerical simulations. The results agree well with theory and simulations. Discrepancies with MAGY may be explained by the fact that the alpha values used for the simulations were not the same as those measured in the experiment. In addition, the actual beam is not ideal. There is some velocity spread, radial spread, and beam nonuniformity which were not included in the MAGY simulations. These beam parameters are being added to the MAGY input and the results will be published in a later paper.

It is important to note that very little evidence was found for multi-moding. The gyrotron was stable in the sense that the design mode, at its optimal operating point, was a pure mode, without the presence of any other frequencies. Therefore any competing modes were successfully suppressed by the $TE_{22,6}$ mode.

The highest power achieved in the design mode was slightly more than 1.4 MW at a beam voltage and current of 96 kV and 40 A, which corresponded to a total efficiency of 37 %. Thus the 1.5 MW power level at 39 % efficiency predicted by theory was not attained. There are several reasons which explain why the gyrotron did not operate at full power and efficiency. First, the beam alpha measured by the alpha probe at the highest efficiency point was only 1.33, possibly due to an axial misalignment of the tube. Therefore, not as much transverse energy was available from the electron beam. If the alpha reached the design value for the gun, 1.43, while still operating in the $TE_{22,6}$ mode, the efficiency of the gyrotron would have in theory increased to 39 %. It may have been possible to increase the alpha by lowering the magnetic field at the cathode. However, as seen in the mode map in Figure 3, doing so would have caused the mode to shift to the $TE_{19,7}$ mode. A second reason is due to other beam effects such as velocity spread, radial spread, and nonazimuthally symmetric effects (nonuniform emission and current distribution, as well as misalignment).

We are also planning additional research using a new tube incorporating an internal mode converter. This mode converter includes a dimpled wall radiating launcher and four internal mirrors to convert the $TE_{22,6}$ mode to a free-space Gaussian beam which propagates through a window transverse to the gyrotron axis. This experiment has already been designed and is currently under construction. Eventually this new tube will use voltage depression with a single stage collector to boost the net efficiency to over 50 %.

VI. CONCLUSION

The progress of the 1.5 MW 110 GHz gyrotron experiment at MIT has been reported. The tube has been shown to stably generate over 1.4 MW in 2.6 μs pulses for a beam voltage and current of 96 kV and 40 A, corresponding to an efficiency of around 37 %. The maximum power and efficiency measured was close to the theoretical design of 1.5 MW and 39 %.

Other than the optimized maximum power demonstration, many other design issues were addressed with this experiment. First, the frequencies close to the design mode frequency were measured. Modes were then assigned to these frequencies, which matched very well with the theory. After the modes were properly identified, a mode map was taken by varying the magnetic field near the cavity and cathode. This map made it possible to locate the limits of the design mode and its proximity to possible competing modes. The points of highest efficiency for various modes were identified on the mode map. The magnetic field was then swept to provide a power scan of the three main modes, the $TE_{21,6}$, $TE_{22,6}$, and the $TE_{23,6}$ modes. At the same time, an alpha probe was used to record the beam alpha for these various operating points. The measured alphas were shown to be consistent with the theoretically predicted values, although slightly lower. The alpha was 1.33 at the point of highest efficiency, while the design alpha at the same point was 1.43. The design mode start-up conditions were then examined by varying the beam voltage and current. Finally, the mode content was shown to be consistent with linear start-up theory, which predicted the start-up current contours for the three main modes in terms of alpha and voltage. These results ultimately confirm and validate the gun and cavity designs. The gun cathode was able to produce a high-quality beam at 96 kV and 40 A necessary for the excitation of a pure $TE_{22,6}$ mode in the cavity, although it may be possible that beam quality is responsible for the slight shortfall in the power and efficiency observed relative to the design goals. The cavity design was likewise validated since close to 1.5

MW of stable power was produced in the design mode with high output purity, although operation in the desired mode was limited to alpha values slightly below the design value, due to excitation of a neighboring ($TE_{19,7}$) mode.

The uniformity of the beam produced by the cathode is an important issue which was addressed in a previous experiment [17]. The present gun uses a replacement cathode. Experiments are planned to quantify the quality of this new cathode in terms of the spread in work function. The next step will include an internal mode converter and single staged depressed collector. The new tube, which has been designed and is currently being constructed, should allow for an efficiency increase by using voltage depression. The total efficiency is predicted to surpass 50 % in this internal mode converter configuration.

REFERENCES

[1] R. W. Callis, W. P. Cary, S. Chu, J. L. Doane, R. A. Ellis, K. Felch, Y. A. Gorelov, H. J. Grunloh, J. Hosea, K. Kajiwara, J. Lohr, T. C. Luce, J. J. Peavy, R. I. Pinsker, D. Ponce, R. Prater, M. Shapiro, R. J. Temkin, and J. F. Tooker, "Maturing ECRF technology for plasma control," *Nucl. Fusion*, vol. 43, pp. 1501-1504, 2003.

[2] H. Idei, S. Kubo, T. Shimozuma, M. Sato, K. Ohkubo, Y. Yoshimura, Y. Takita, S. Kobayashi, S. Ito, Y. Mizuno, K. Tsumori, K. Ikeda, T. Notake, T. Watari, O. Kaneko, A. Komori, H. Yamada, P. C. de Vries, M. Goto, K. Ida, S. Inagaki, S. Kado, K. Kawahata, T. Kobuchi, T. Minami, J. Miyazawa, T. Morisaki, S. Morita, S. Murakami, S. Muto, Y. Nagayama, H. Nakanishi, K. Narihara, B. J. Peterson, S. Sakakibara, H. Sasao, K. Sato, K. Tanaka, Y. Takeiri, K. Y. Watanabe, I. Yamada, O. Motojima, M. Fujiwara, and LHD Experimental Group, "Electron cyclotron heating scenario and experimental results in LHD," Fusion Engineering and Design, vol. 53, pp. 329-336, 2001.

[3] K. Kajiwara, Y. Ikeda, K. Sakamoto, A. Kasuqai, M. Seki, S. Moriyama, K. Takahashi, T. Imai, Y. Mitsunaka. T. Fujii, "High power operation of 110 GHz gyrotron at 1.2 MW on the JT-60 ECRF system," *Fusion Engineering and Design*, vol. 65, no. 4, pp. 493-499, July, 2003.

[4] J. P. Hogge, S. Alberti, L. Porte, and G. Arnoux, "Preliminary results of top launch third harmonic X-mode electron cyclotron heating in the TCV tokamak," *Nucl. Fusion*, vol. 43, pp. 1353-1360, 2003.

[5] F. Leuterer, R. Dux, G. Gantenbein, J. Hobirk, A. Keller, K. Kirov, M. Maraschek, A. Muck, R. Neu, A. G. Peeters, G. Pereverzev, F. Ryter, J. Stober, W. Suttrop, G. Tardini, H. Zohm, and AUG Team, "Recent ECRH results in ASDEX Upgrade," *Nucl. Fusion*, vol. 43, pp. 1329-1342, 2003.

[6] G. Dammertz, S. Alberti, A. Arnold, E. Borie, V. Erckmann, G. Gantenbein, E. Giguet, R. Heidinger, J. P. Hogge, S. Illy, W. Kasparek, K. Koppenburg, M. Kuntze, H. Laqua, G. LeCloarec, F. Legrand, Y. LeGoff, W. Leonhardt, C. Lievin, R. Magne, G. Michel, G. Muller, G. Neffe, B. Piosczyk, M. Schmid, M. Thumm, M.Q. Tran, "Progress in the development of a 1-MW gyrotron at 140 GHz for fusion plasma heating," in *Fourth IEEE Int'l Vacuum Elect. Conf.* Piscataway, NJ: IEEE, 2003, pp. 34-35.

[7] T. S. Chu, M. Blank, P. Borchard, P. Cahalan, S. Cauffman, K. Felch, and H. Jory, "Development of high power gyrotrons at 110 GHz and 140 GHz," in *Fourth IEEE Int'l Vacuum Elect. Conf.* Piscataway, NJ: IEEE, 2003, pp. 32-33.

[8] K. Felch, M. Blank, P. Borchard, P. Cahalan, S. Cauffman, T. S. Chu, and H. Jory, "Progress update on CPI 500 kW and 1 MW, multi-second-pulsed gyrotrons," in *Third IEEE Int'l Vacuum Elect. Conf.* Piscataway, NJ: IEEE, 2002, pp. 332-333.

[9] T. Imai, N. Kobayashi, R. Temkin, M. Thumm, M. Q. Tran, and V. Alikaev, "ITER R&D: Auxiliary systems: Electron cyclotron heating and current drive system," *Fusion Engineering and Design*, vol. 55, Issues 2-3, pp. 281-289, July 2001.

[10] R. Advani, D. Denison, K. E. Kreischer, M. A. Shapiro, R. J. Temkin, "Multimegawatt gyrotrons for plasma heating," in *26th Int'l Conf. on Plasma Sci.* Piscataway, NJ: IEEE, 1999, p. 162.

[11] A. Singh, S. Rajapatirana, Y. Men, V. L. Granatstein, R. L. Ives, and A. J. Antolak, "Design of a multistage depressed collector system for 1-MW CW gyrotrons—Part 1: Trajectory control of primary and secondary electrons in a two-stage depressed collector," *IEEE Trans. Plasma Sci.*, vol. 27, no. 2, pp. 490-502, April 1999.

[12] M. Kuntze, S. Alberti, G. Dammertz, E. Giguet, S. Illy, R. Hedidinger, K. Koppenburg, G. LeCloarec, Y. LeGoff, W. Leonhardt, B. Piosczyk, M. Schmid, M. Thumm, and M. Q. Tran, "Advanced high-power gyrotrons," *IEEE Trans. Plasma Sci.*, vol. 31, no. 1, pp. 25-31, Feb. 2003.

[13] K. Sakamoto, A. Kasugai, Y. Ikeda, K. Hayashi, J. Takahashi, M. Tsuneoka, T. Kariya, Y. Mitsunaka, and T. Imai "Development of 170 GHz and 110 GHz gyrotron for fusion application," in *Third IEEE Int'l Vacuum Elect. Conf.* Piscataway, NJ: IEEE, 2002, pp. 336-337.

[14] V. A. Flyagin, V. I. Khizhnyak, V. N. Manuilov, M. A. Moiseev, A. B. Pavelyev, V. E. Zapevalov, and N. A. Zavolsky, "Investigations of advanced coaxial gyrotrons at IAP RAS," *Int. J. Infrared Millim. Waves*, vol. 27, no. 1, pp. 1-17, Jan. 2003.

[15] K. E. Kreischer, T. Kimura, B. G. Danly, and R. J. Temkin, "High-power operation of a 170 GHz megawatt gyrotron," *Phys. Plasmas*, vol. 4, no. 5, pp. 1907-1914, May 1997.

[16] J. P. Anderson, M. A. Shapiro, R. J. Temkin, and I. Mastovsky, "Initial results from the 1.5 MW, 110 GHz gyrotron experiment at MIT," in *27th Int'l Conf. on Millimeter Waves*. Piscataway, NJ: IEEE, 2002, pp. 11-12.

[17] J. P. Anderson, S. E. Korbly, R. J. Temkin, M. A. Shapiro, K. L. Felch, and S. Cauffman, "Design and emission uniformity studies of a 1.5-MW gyrotron electron gun," *IEEE Trans. Plasma Sci.*, vol. 30, no. 6, pp. 2117-2123, Dec. 2002.

[18] W. B. Hermannsfeldt, "Electron trajectory program," Technical Report SLAC-226, UC-28, Stanford Linear Accelerator Center, Nov. 1979.

[19] A. W. Fliflet, "Linear and nonlinear theory of the doppler-shifted cylcotron resonance maser based on TE and TM waveguide modes," *Int'l Journal of Elec.,* vol. 61, no. 6, pp. 1049-1080, Dec. 1986.

[20] M. Botton, T. M. Antonsen Jr., B. Levush, A. Vlasov, and K. Nguyen, "MAGY: A time dependent code for simulation of electron beam devices," *IEEE Trans. Plasma Sci.*, vol. 26, no. 3, pp. 882-892, June, 1998.

[21] W. C. Guss, T. L. Grimm, K. E. Kreischer, J. T. Polevoy, and R. J. Temkin, "Velocity ratio measurements of a gyrotron electron beam," *J. Appl. Phys.*, vol. 69, no. 7, pp. 3789-3795, April 1991.

[22] G. S. Nusinovich, A. N. Vlasov, M. Botton, T. M. Antonsen, Jr., S. Cauffman, and K. Felch, "Effect of the azimuthal inhomogeneity of electron emission on gyrotron operation," *Phys. Plasmas*, vol. 8, no. 7, p. 3473-3479, 2001.